ARCHIVES OF ACOUSTICS
23, 2, 251–266 (1998)

ACOUSTICAL DISTORTIONS IN CAPACITANCE HYDROPHONES AND THE EFFECT OF DIAPHRAGMS IN MEASUREMENTS OF SHOCK WAVE PULSES

L. FILIPCZYŃSKI, J. ETIENNE, T. KUJAWSKA, J. WÓJCIK, B. ZIENKIEWICZ

Department of Ultrasound,
Institute of Fundamental Technological Research,
Polish Academy of Sciences
(00-049 Warszawa, ul. Świętokrzyska 21)

The shock wave pulse measured by means of a membrane PVDF hydrophone was compared with the pulse obtained by means of the capacitance hydrophone showing distortions in the pulse trailing edge. The mechanism of distortions in the capacitance hydrophone was explained and confirmed by experiments as caused by transverse waves generated on the surface of the hydrophone's metal plate by compressional incident waves. The effect of the rise time of the measured shock wave pulses was interpreted and analysed by means of diaphragms with various apertures. Interaction of the applied diaphragms with the measured acoustic fields was explained showing their equivalence to the high pass filtering. The differentiating circuit used for determination of the particle velocity from the displacement, measured by the capacitance hydrophone, was analysed. Also an improved capacitance hydrophone was applied in measurements.

1. Introduction

The capacitance hydrophone for measurements in liquids was described first in 1969 [3]. In a later paper [7], a capacitance hydrophone for measurements of shock wave pulses and its multiple applications in lithotripsy [5, 8, 9, 10] were described. Some of its advantages like large durability and direct calibration based on electrical measurements were shown. On the other hand, the capacitance hydrophone deforms mainly the trailing edge of the measured shock wave pulse. Therefore, its application is limited to measurements of the leading edge in the direct vicinity of the pulse peak, to measurements of the positive peak pressure, and to measurements of only the first portion of the pulse trailing edge. In the mentioned paper [7] it was found that the distortions of the pulse trailing edge are caused by transverse waves arising in the metal front plate of the hydrophone. This statement was proved by measuring the speed of the wave arising in the front plate. However, at that time the authors could not explain the reasons of this interfering effect. The purpose of the present paper is to give an exact explanation of acoustical distortions arising in capacitance hydrophones supported by experiments, as well as to present a modified hydrophone's version which makes it possible to limit the described distortions.

2. The capacitance hydrophone

Figure 1 shows the principle of the capacitance hydrophone [7]. The incident ultrasonic pulse penetrates into the metal front plate and changes the capacitance formed by the electrically polarized electrode E with respect to the metal front plate. In such a case, on the electrode terminals there arises an electrical signal e which is proportional to the displacement of the incident wave. The pressure p of this wave can be found by means of the formula

$$p = \frac{d_0(\varrho_p c_p + \varrho_w c_w)(C_0 + C')}{4C_0 U_0} \frac{de}{dt}, \tag{1}$$

where d_0 denotes the thickness of the air gap between the electrode E and the metal front plate P, $\varrho_p c_p$, $\varrho_w c_w$ – acoustic impedances of the plate material and water, C_0, C' – electrode capacity and stray capacity, respectively, U_0 – polarizing voltage, e – measured electrical signal, t – time. Equation (1) is valid for the condition $\xi \ll d_0$, where ξ is displacement.

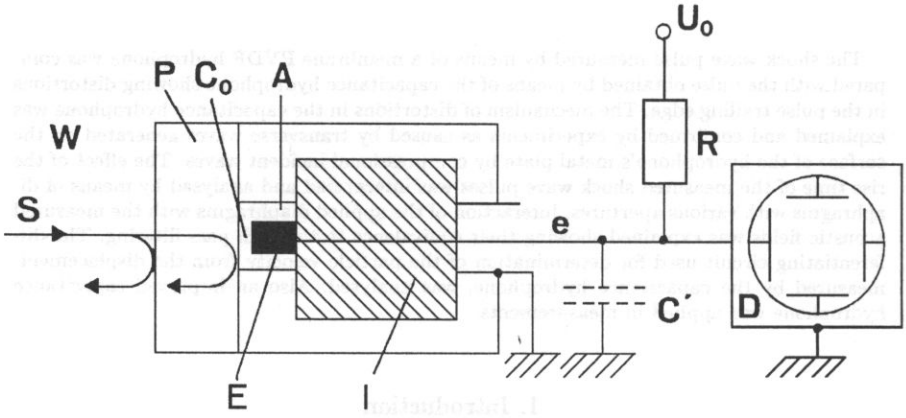

Fig. 1. The principle of the capacitance hydrophone. S – incident shock wave pulse, W – water, P – metal front plate, E – electrode, C_0 – electrode capacity, A – air cavity, I – insulator, e – measured signal, C' – stray capacity, U_0 – polarizing voltage, R – separating resistor, D – digital memory oscilloscope.

In Eq. (1) a linear dependence was assumed between the acoustic pressure p and the particle velocity v, where $v = d\xi/dt$. In our case of nonlinear fields, it is satisfied with a sufficient accuracy [6, 2].

The shape of the shock wave pressure pulse (or particle velocity pulse) used in lithotripsy, measured by means of a distortionless, however undurable PVDF membrane hydrophone in water, is shown in Fig. 2. In Fig. 3 is presented the corresponding displacement pulse $\xi(t)$ obtained by means of numerical integration of the pulse from Fig. 2 according to the relation

$$\xi = \int v\, dt \tag{2}$$

where $v(t)$ denotes the pulse of particle velocity.

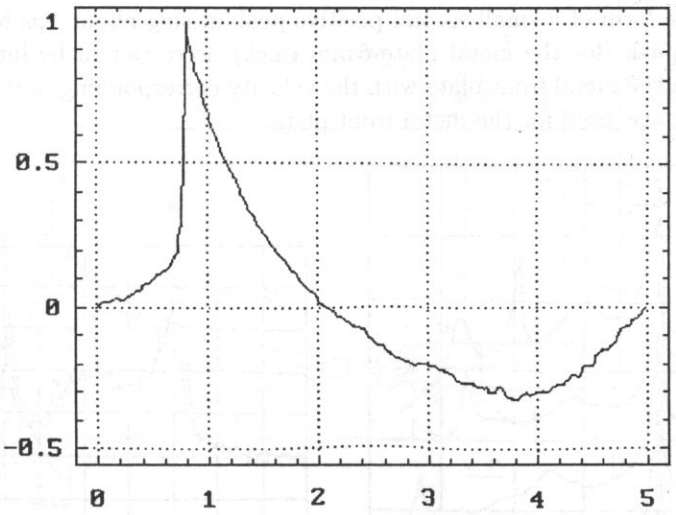

Fig. 2. Shape of the shock wave pulse with the peak positive pressure of 20 MPa measured in the focal distance of our lithotripter in water by means of the membrane PVDF hydrophone. Vertical scale – relative units, horizontal scale – μs.

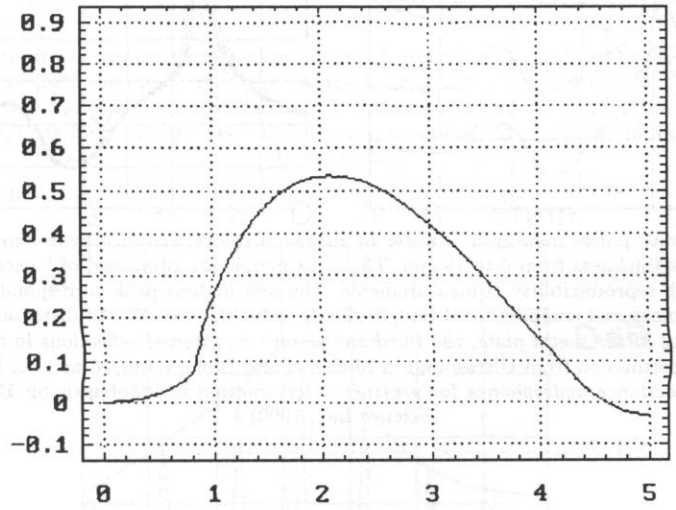

Fig. 3. Shock wave pulse of displacement $\xi(t)$ computed from the pulse from Fig. 2. Vertical scale – relative units, horizontal scale – μs.

Due to properties of the PVDF membrane hydrophone [13] one can assume that the obtained shape of the pulse corresponds exactly to the real pressure or particle velocity pulse obtained in the lithotripsy system under investigations. The same pulse shape was obtained when using the electromagnetic hydrophone recently developed [2].

On the other hand, the same lithotripsy pulse measured with the capacitance hydrophone shows distortions of its trailing edge as can be seen in Fig. 4 [7]. These dis-

tortions, in the form of a small second positive peak arising about 1 μs behind the first positive high peak (for the metal plate 6 mm thick), were caused by interfering waves propagating in the metal front plate with the velocity corresponding to transverse waves in steel, which was used for the metal front plate.

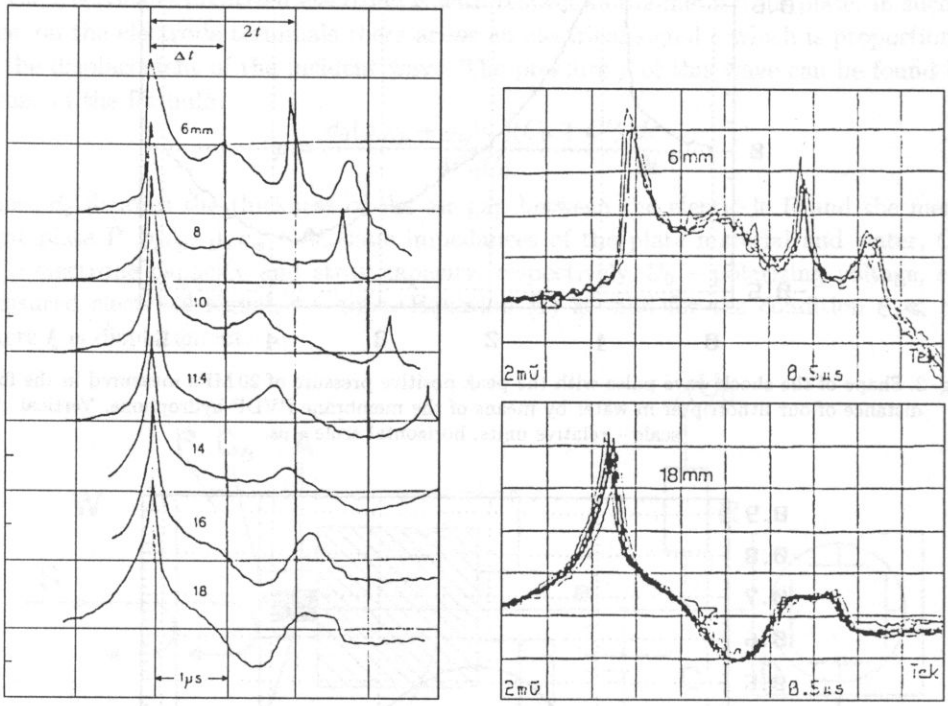

Fig. 4. Shock wave pulses measured in water by means of the capacitance hydrophone with various steel front plate thickness from 6 to 18 mm. The right figures are composed of 5 successive patterns to show the high reproducibility of measurements. The first highest peak corresponds to the highest value of the measured compressional (longitudinal) wave, the second – to distortions caused by transverse waves in the metal plate, the third and so on – to internal reflections in the metal plate (reprinted with permission from Ultrasound in Medicine and Biology, vol. 16 no 1, L. Filipczyński and J. Etienne, *Capacitance hydrophones for pressure determination in lithotripsy*, pp. 157–165, Elsevier Science Inc., 1990).

3. The mechanism of distortions in the capacitance hydrophone

There arises a question of how it is possible to explain the generation of transverse waves in the hydrophone when the incident wave is a compressional (longitudinal) one. To answer this question, many experiments were carried out with additional diaphragms situated in front of the hydrophone (Fig. 5). The transverse pressure distribution of the incident wave beam shows its nonuniformity as presented in Fig. 6. So one can consider the propagation of the beam as a set of parallel rays, propagating along the path r with amplitudes and phases depending on the distance from the symmetry axis of the beam.

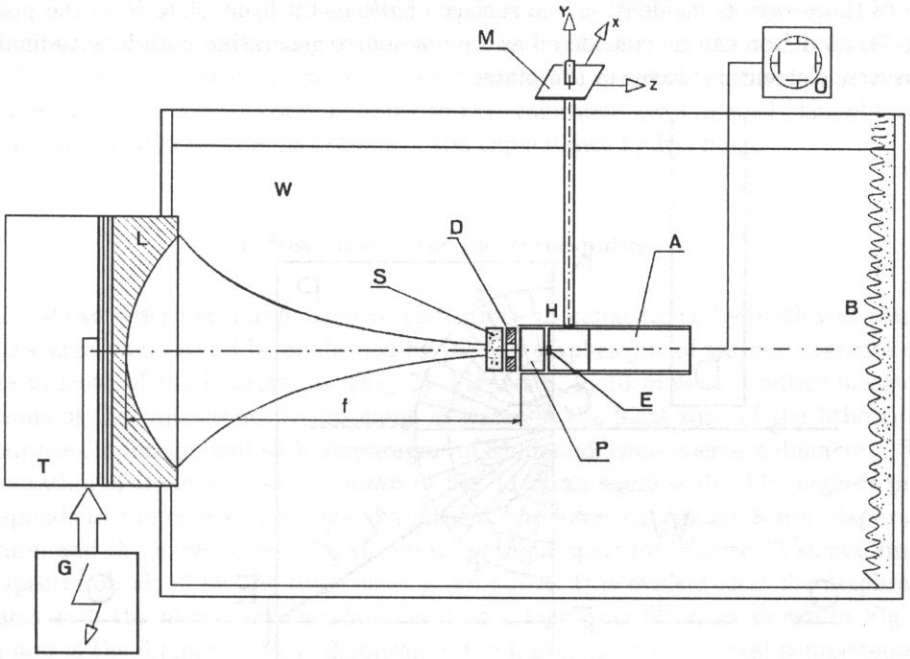

Fig. 5. The lithotripsy system with the measurement unit of capacitance hydrophone H and the diaphragm D. P denotes the metal front plate of the hydrophone, E – its electrode, S – tissue sample, A – amplifier, O – digital memory oscilloscope, T – electromagnetic membrane shock wave source, L – plastic lens, f -its focal distance, G – high voltage generator, M – microscope table, W – water, B – absorber.

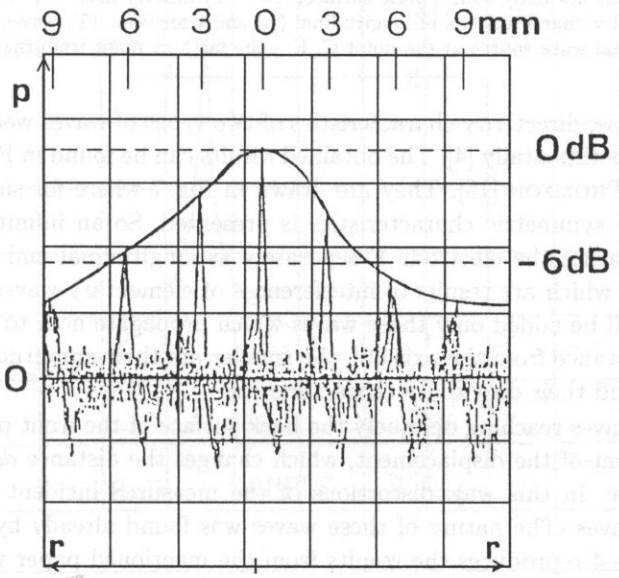

Fig. 6. Transverse distribution of shock wave pulses measured in water in the focus of the ultrasonic beam used in lithotripsy. Vertical scale – relative units, horizontal axis – radial coordinate in mm.

One of those rays is incident on the surface of the metal front plate P at the point C (Fig. 7). Its action can be considered as a point source generating both longitudinal and transverse elementary waves in the plate.

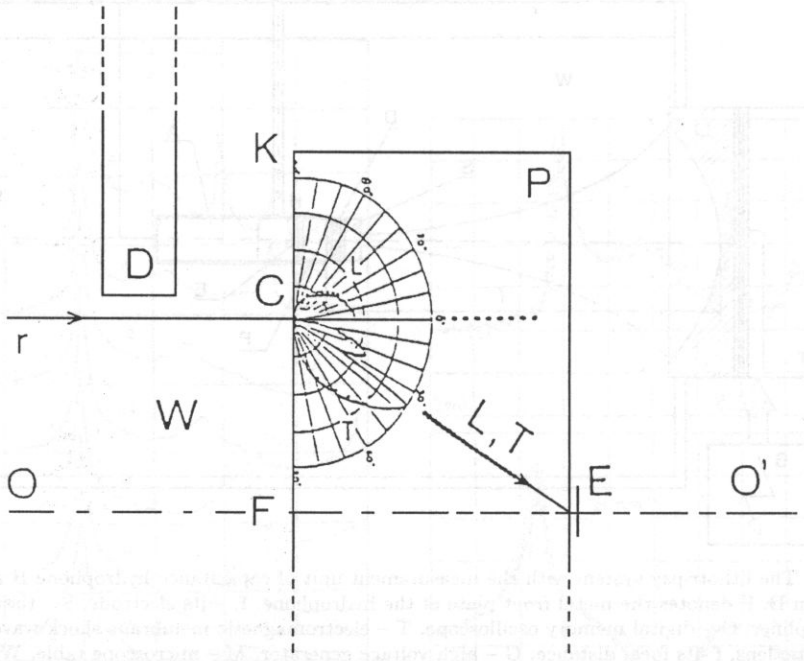

Fig. 7. The capacitance hydrophone with the diaphragm D in front of the metal plate P. r denotes an acoustic ray incident normally to the plate surface, OO' – symmetry axis, W – water, E – electrode, L, T – directivity characteristics of longitudinal (L) and transverse (T) waves generated by a longitudinal wave source at the point C, K – the farthest point from the OO' axis.

For such a case, directivity characteristics of two types of waves were found theoretically [16] and experimentally [4]. The obtained results can be found in Physical Acoustics of MASON and THOMSON [15]. They are drawn in Fig. 7 where for simplification, only one half of their symmetric characteristics is presented. So an infinite number of elementary rays reaches the electrode E seperately as longitudinal and transverse waves with amplitudes which are results of interferences of elementary waves. One can notice that in phase will be added only those waves which propagate near to the axis $00'$. The greater is the distance from the axis $00'$, the smaller are their amplitudes due to greater phase changes and their directivity characteristics.

Transverse waves reaching obliquely the back surface of the front plate P generate a normal component of the displacement, which changes the distance d_0 of the electrode E from the plate. In this way, distortions of the measured incident pulse are caused by transverse waves. The nature of these waves was found already by measuring their speed [7]. Figure 4 reproduces the results from the mentioned paper where shock-wave pulses and their distortions were shown in the capacitance hydrophone, when increasing the thickness of the steel front plate from 6 mm to 18 mm. Distortions occur from 1 μs

to 2.3 μs behind the main positive peak, depending on the plate thickness. The next positive sharp peak corresponds to the second inner reflection in the hydrophone steel plate. In this experiment it was possible to determine the speed of the interfering wave in the plate equal to 3.3 km/s corresponding to the transverse wave in steel. The obtained patterns show distinctly the limitations of the capacitance hydrophone.

4. Rise time of the measured pulses

The above described mechanism of distortions in capacitance hydrophones caused by transverse waves could be confirmed by placing diaphragms of various aperture diameters in front of the hydrophone (Fig. 7). Figures 8, 9, 10 present 3 pulses measured by means of the capacitance hydrophone in water in the focal zone of the lithotripter without the diaphragm and with diaphragms of 8 mm and 5 mm aperture diameters. The confrontation of these 3 pulses is shown in Fig. 11 in an equal scale. The highest pulse corresponds to the case without the diaphragm, the lower one to the 8 mm diaphragm aperture, and the lowest one to the 5 mm diaphragm aperture. Figure 12 shows amplitude spectra obtained for the three cases given above. It is evident that the diaphragm interacts with the plane wave incident on it as a high pass filter, as shown in Fig. 12. The lower is the diameter of the diaphragm, the higher are the spectral components of the beam penetrating the diaphragm. This effect will be explained in details in Sec. 6.

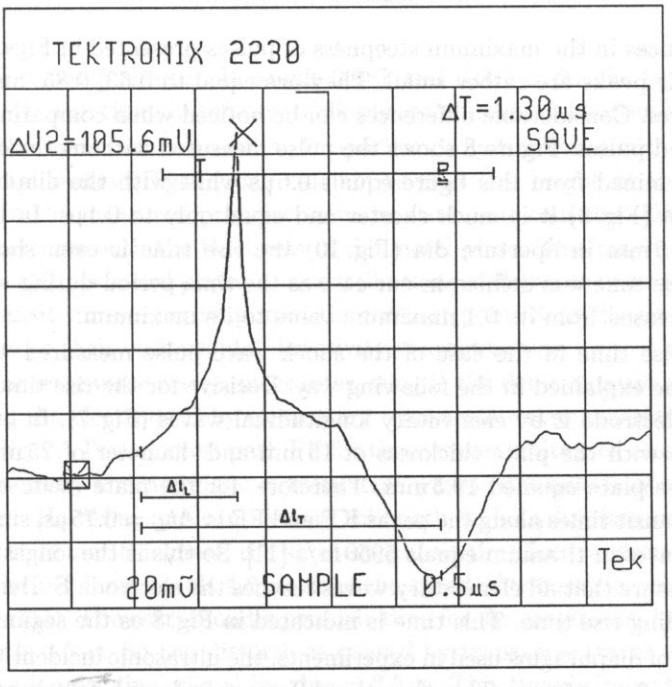

Fig. 8. Shock wave pulse measured without the diaphragm. Vertical scale – relative units, horizontal scale – 0.5 μs.

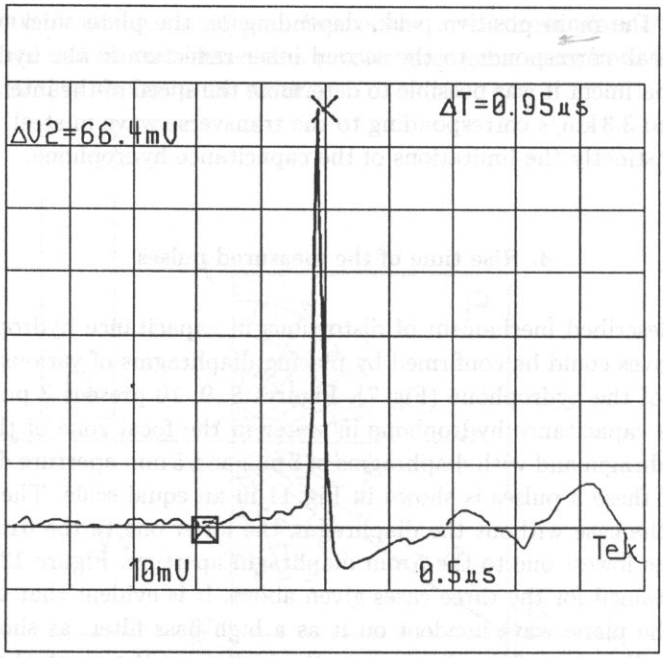

Fig. 9. Shock wave pulse measured with the diaphragm of 8 mm in aperture dia. Vertical scale – relative units, horizontal scale – 0.5 μs.

The differences in the maximum steepness of pulses presented in Figs. 8, 9, 10 in the vicinity of their peaks are rather small. They are equal to 0.63, 0.85, and 0.60 V/μs in all of these cases. Considerable differences can be noticed when comparing the rise time of the measured pulses. Figure 8 shows the pulse measured without the diaphragm, the rise time determined from this figure equals 0.6 μs while with the diaphragm of 8 mm in aperture dia (Fig. 9) it is much shorter and equal only to 0.1 μs. In the case of the diaphragm of 5 mm in aperture dia (Fig. 10) the rise time is even shorter, it equals 0.06 μs. The rise time was defined in our case as the time period during which the pulse amplitude increased from its 0.1 maximum value to its maximum.

The long rise time in the case of the shock wave pulse measured without the diaphragm can be explained in the following way. Decisive for the rise time is the time of reaching the electrode E by elementary longitudinal waves (Fig. 7). In our new version of hydrophone with the plate thickness of 15 mm and diameter of 25 mm, the longest path KE in the plate equaled 19.5 mm. Therefore, for the plate made of titanium the difference in transit times along the paths KE and FE is $\Delta t_L = 0.75$ μs, since the speed of longitudinal waves in titanium equals 5950 m/s [11]. So this is the longest time which is necessary to assure that all elementary waves reaches the electrode E. Hence one obtains the corresponding rise time. This time is indicated in Fig. 8 as the segment Δt_L.

In the case of diaphragms used in experiments, the ultrasonic incident beam is limited in diameters to 8 and 5 mm. Therefore the difference in length for elementary longitudinal wave paths CE and FE (Fig. 7) and the corresponding time difference in reaching

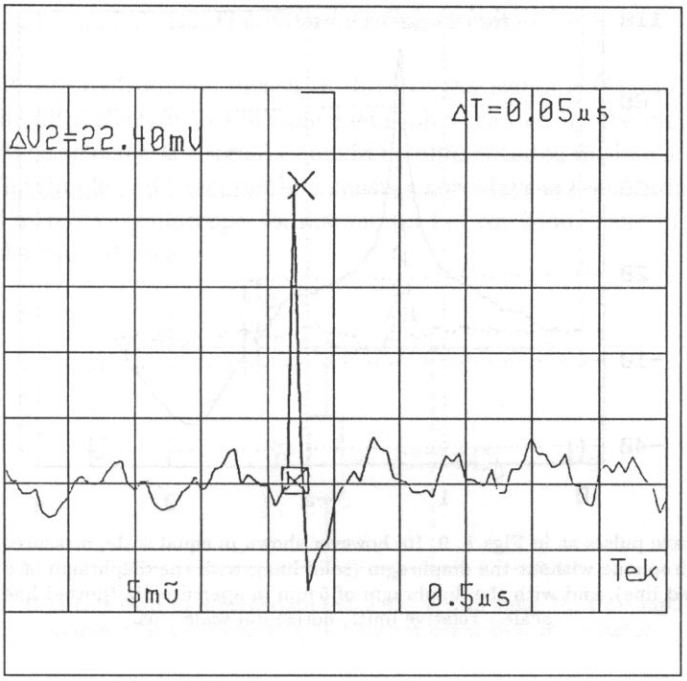

Fig. 10. Shock wave pulse measured with the diaphragm of 5 mm in aperture dia. Vertical scale – relative units, horizontal scale – 0.5 μs.

the electrode E is much shorter. It equals 0.087 and 0.035 μs for the two diaphragms, respectively. So the rise times in the case of diaphragms are much shorter, as given above.

Observing the measurement results of capacitance hydrophones with various thickness of the metal plates (Fig. 4), one can notice that the height of the first peak – corresponding to the measured pressure value in water – is constant. On the contrary, the rise time increases with the thickness of the metal plate. This may be explained by the fact that for thinner metal plates, the contributions of elementary longitudinal waves with longest transit times – arriving from the farthest point K to the point E (Fig. 7) – tend to zero due to their cosinusoidal directivity characteristics.

In the case of transverse waves, most interesting is the determination of the shortest time of reaching the electrode E by elementary transverse waves generated at the plate front surface (Fig. 7). The shortest path FE for these waves is situated along the axis $00'$. In fact, the directivity characteristic of transverse waves does not show any component in this direction. However, one can assume this path to be a limiting case. So for the titanium plate of 15 mm thickness, the shortest transit time for transverse waves in our new version of hydrophone equals 4.8 μs, since the speed of transverse waves in titanium equals 3120 m/s [11]. The corresponding transit time for the longitudinal wave along the same path equals 2.5 μs. So the distortions caused by transverse waves will be delayed in respect of the longitudinal signal by $\Delta t_T = 2.3\,\mu s$. This time is indicated in Fig. 8 as the segment Δt_T.

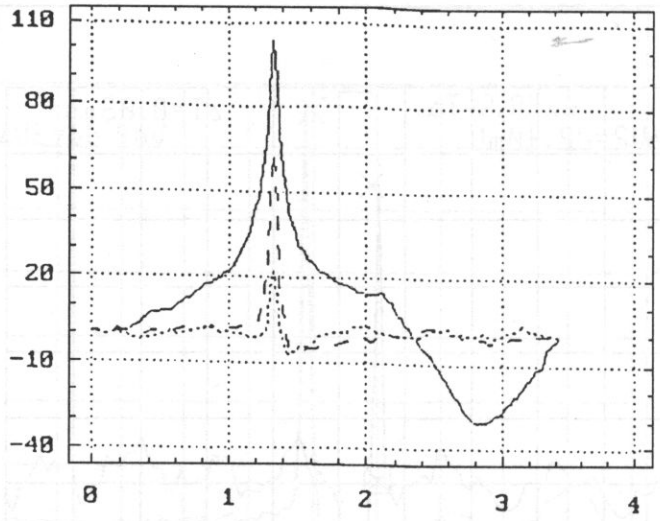

Fig. 11. Shock wave pulses as in Figs. 8, 9, 10, however shown in equal scale, measured by means of the capacitance hydrophone without the diaphragm (solid line), with the diaphragm of 8 mm in aperture dia (dashed line), and with the diaphragm of 5 mm in aperture dia (dotted line). Vertical scale – relative units, horizontal scale – μs.

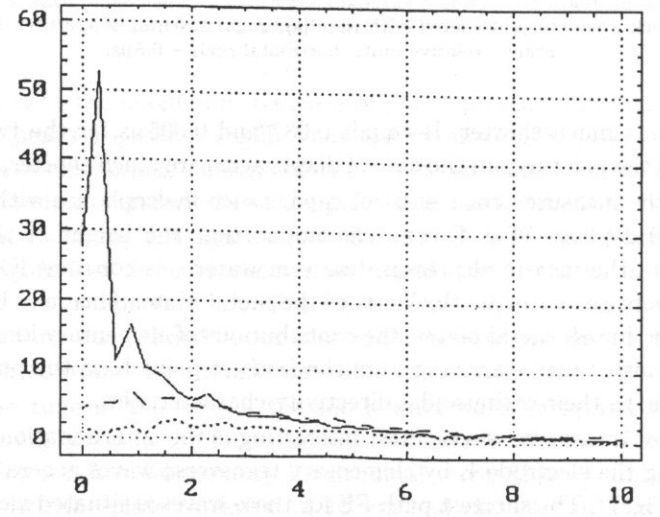

Fig. 12. Amplitude spectra of shock wave pulses shown in Fig. 11 without the diaphragm (solid line), with the diaphragm of 8 mm in aperture dia (dashed line), and with the diaphragm of 5 mm in aperture dia (dotted line). Vertical scale – relative units, horizontal scale – MHz.

Hence the following conclusion valid for our capacitance hydrophone can be drawn. Transverse waves do not interfere in the time period equal to $\Delta t_T = 2.3\,\mu s$ after the first signal received. Therefore, in our last measurements this type of improved version of the capacitance hydrophone was applied.

5. The differentiating circuit

The capacitance hydrophone measures directly the signal e (Fig. 1), which is proportional to the displacement in the front metal plate caused by the incident wave. To obtain the particle velocity, the signal e should be differentiated in time according to the formula (1). The simple and exact method consists nowadays in registration of the signal e in the digital memory oscilloscope, for instance in LeCroy 9450A, and in differentiating it directly in the same device.

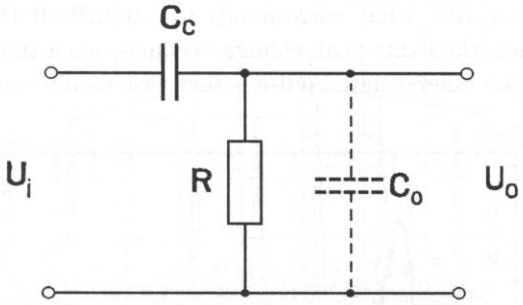

Fig. 13. The RC circuit used to differentiate the signal $e(t)$ in time. U_i, U_o – input and output voltages, C_C, C_0 – coupling and output capacities, R – resistor.

However, in our previous works [5], to observe the measured particle velocity in real time we used for this purpose a simple differentiating circuit shown in Fig. 13 where the relation $2\pi fRC \ll 1$ should be fulfilled, f is here the frequency. In that case when $U_o(t)$ denotes the output voltage at the circuit terminals, one obtains the expression

$$\frac{de(t)}{dt} = \frac{U_o(t)}{RC} \tag{3}$$

which can be directly inserted into the formula (1) expressing the value of the measured pressure. However, the capacity C_0 at the output of the circuit (Fig. 13), composed mainly of the input capacity of the following amplifier or oscilloscope, complicates the situation. It is evident that it may decrease the high frequency spectral components of the measured pulse. In our measurements we used the values $C_C = 24\,\mathrm{pF}$ and $R = 1.9\,\mathrm{k\Omega}$. The value of $C_0 = 20\,\mathrm{pF}$ was determined by means of continuous wave measurements. The transfer function β of the circuit under discussion equals

$$\beta(f) = \frac{U_i}{U_o} = \frac{j2\pi fRC_C}{1 + j2\pi f(RC_0 + RC_C)} \tag{4}$$

where U_i, U_0 denote the input and output voltages at the circuit terminals.

Hence one can determine the shape and the value of the differentiated input pulse $e(t)$ being equal to the particle velocity $v(t)$. Using the inverse Fourier transform of the product of the amplitude spectrum of the incident displacement pulse $e(t)$ and the complex transfer function $\beta(f)$ [1], one obtains

$$v(t) = \frac{de(t)}{dt} = \mathbf{F}^{-1}\{\mathbf{F}[e(t)] \cdot \beta(f)\} \tag{5}$$

where $\mathbf{F}$ and $\mathbf{F}^{-1}$ are Fourier and inverse Fourier transforms.

In the procedure (5), first the wave pulse $e(t)$ is transformed into the frequency domain. Then every frequency component was multiplied by the corresponding value of the transfer function $\beta(f)$. Finally the inverse Fourier transform of the result was computed to synthesize the resulting pulse shape.

Figure 14 shows the results obtained by means of the procedure (5) presenting the pulses at the output of the differentiating circuit, assuming at its input the displacement pulse $e(t)$ in the form as shown in Fig. 3. It follows from the results that the output capacity C_0 causes a small change of the measured pulse shape, mainly decreasing its positive peak by about 10% what corresponds to $-0.9\,\mathrm{dB}$. If the resistor R will be decreased several times, then this peak change becomes much smaller. The decrease of the absolute value of the differentiated pulse is then practically compensated by the RC value in Eq. (3).

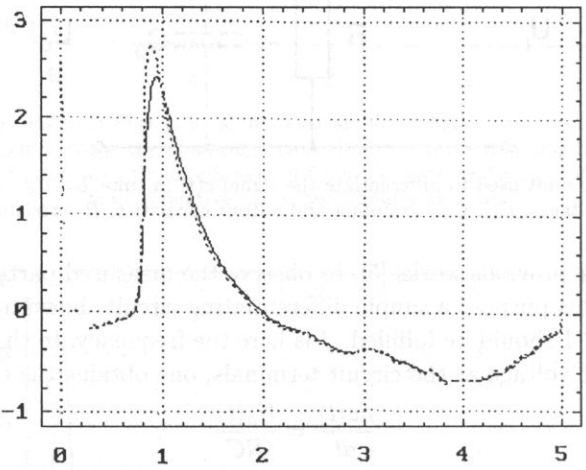

Fig. 14. Shock wave pulse of particle velocity $v(t)$ after differentiating of the displacement pulse $e(t)$ from Fig. 3 by the RC circuit for $C_0 = 20\,\mathrm{pF}$ (solid line) and $C_0 = 0$ (dotted line). The other values are $C_C = 24\,\mathrm{pF}$ and $R = 1.9\,\mathrm{k\Omega}$.

Hence one can conclude that the output capacity C_0 causes the decrease of the positive peak value by about 10% and has no influence on other portions of the measured pulse. So our previous results obtained by means of our capacitance hydrophone with the differentiating circuit [5, 7, 8, 9] can be considered to be practically correct, although the measured positive peak pressures were a little lower than those in reality.

6. The influence of diaphragms on the shock wave pulse

The diaphragm inserted into the path of the propagating shock wave pulse can be considered as a high pass filter. According to our previous measurements [7] and our actual measurements presented in Fig. 15, one can assume the propagating wave in the focal region to be plane. In such a case, a soft aperture in the diaphragm forms an input impedance for the wave which can be considered to be approximately [12] equal to the

input impedance of a rigid piston in an infinite screen. The magnitude and the phase of such an impedance is shown in Fig. 16 as adapted from the book of MALECKI [14]. One can see that the input impedance of the aperture equals ϱc for higher ka values; it means a perfect matching of the media on both sides of the aperture, assuring a perfect penetration of the wave. For lower ka values the input impedance of the aperture becomes lower than ϱc, therefore one obtains a mismatch and the incident wave can not penetrate the aperture.

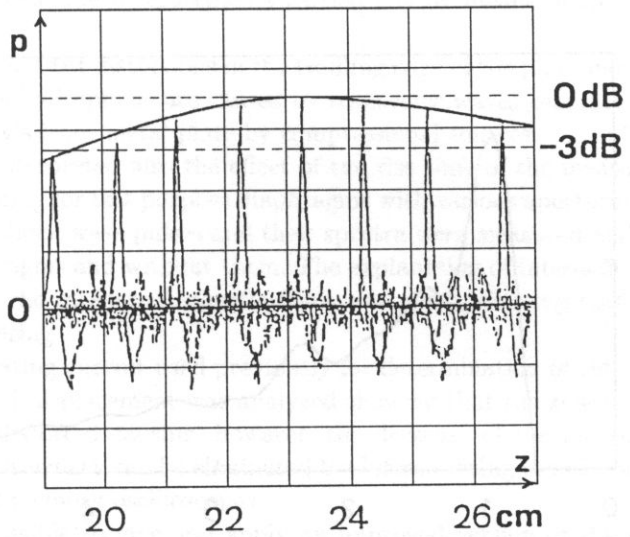

Fig. 15. Axial distribution of shock wave pulses measured in water in the focal region of the ultrasonic beam used in lithotripsy. Vertical scale – relative units, horizontal scale – axial coordinate z in cm.

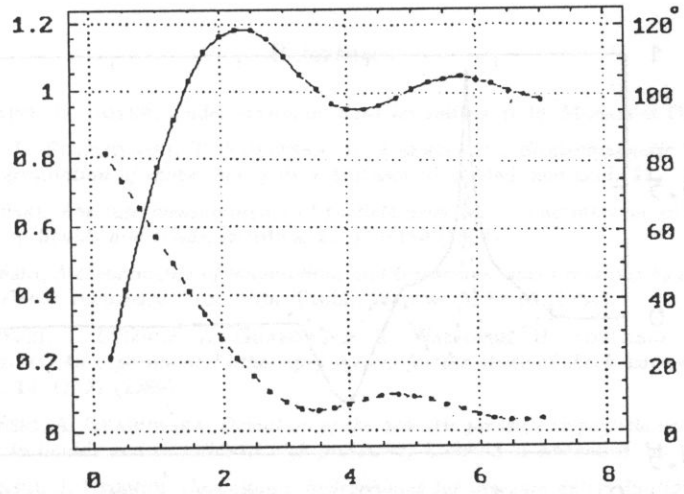

Fig. 16. The magnitude (solid line) and the argument (dashed line) of the relative input impedance $Z/\varrho c$ of a piston in an infinite screen as a function of ka where $k = 2\pi f/c$ and a denotes the piston radius.

This rather qualitative conclusion can be confirmed by removing from the full spectrum (Fig. 9) of the shock wave pulse (measured without the diaphragm) the low frequency components from 0 to 0.6 MHz. The resulting limited spectrum is shown in Fig. 17 and the shock wave pulse synthesized from it is presented in Fig. 18. One can notice that the pulse obtained in this way becomes similar to the shock wave pulse from Fig. 8 (dashed line) measured with the 8 mm diaphragm aperture. So it is evident that the diaphragm interaction with the shock wave pulses is equivalent to the high pass filtering.

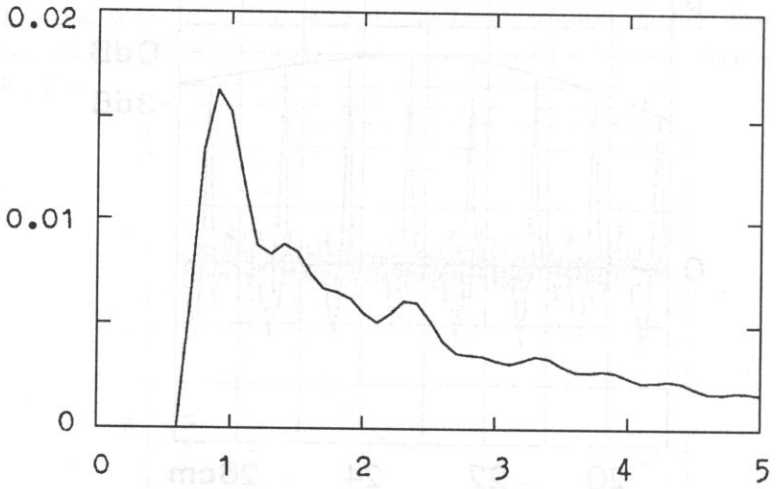

Fig. 17. The amplitude spectrum of the shock wave pulse measured without the diaphragm after removing of spectral components with frequencies from 0 to 0.6 MHz. Vertical scale – relative units, horizontal scale – MHz.

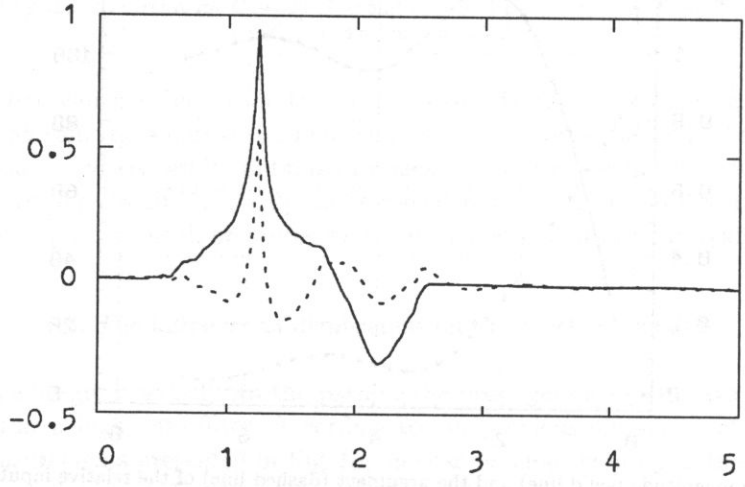

Fig. 18. Shock wave pulses measured without diaphragm (full line) and computed from the spectrum shown in Fig. 17. Vertical scale – relative units, horizontal scale – μs.

7. Conclusions

The mechanism of distortions occurring in capacitance hydrophones was explained and confirmed by experiments. For this purpose the ultrasonic field in the case of lithotripsy was measured in the focal region showing its radial and also axial distributions. Basing on the shock wave pulse measured in water by means of a distortionless, however undurable membrane PVDF hydrophone, it was possible to compare the obtained results with the measurements carried out by means of the capacitance hydrophone.

It was shown that the distortions in the trailling edge of the pulse measured by means of the capacitance hydrophone are caused by transverse waves generated on the surface of the hydrophone's front metal plate by compressional sources.

The authors interpreted also the effect of the rise time of the measured shock wave pulses by introducing for this purpose diaphragms with various apertures. To explain the obtained effects, shock wave pulses and their spectra were measured and interpreted for the case of diaphragms and without them. The explanation of interaction of the applied diaphragms with the measured acoustic fields was given, showing their equivalence to the high pass filtering.

The differentiating curcuit used previously for determination of the particle velocity from the measured displacement was analyzed showing that the shape of the measured pulses were not distorted causing, however, the decrease of the measured peak value about 10%. This drawback can be eliminated by differentiating the displacement directly in modern digital memory oscilloscopes.

It was also possible to give and apply an improved version of the capacitance hydrophone with a thicker titanium front plate which limits the distortions introduced by transverse waves generated in this plate.

References

[1] E. DIEULESAINT, D. ROYER, *Ondes elastiques dans les solides*, p. 36, Masson et Cie, Paris 1974.

[2] J. ETIENNE, L. FILIPCZYŃSKI, T. KUJAWSKA, B. ZIENKIEWICZ, *Electromagnetic hydrophone for pressure determination of shock wave pulses*, Ultrasound in Med. and Biol., **23**, 747–754 (1997).

[3] L. FILIPCZYŃSKI, *Absolute measurements of particle velocity, displacement or intensity of ultrasonic pulses in liquids and solids*, Acustica, **21**, 173–180 (1969).

[4] L. FILIPCZYŃSKI, *Measurements of longitudinal and transverse waves radiated by a compressional source into elastic semispace*, Proc. Vibr. Probl., Warsaw, 5, 89–93 (1964).

[5] L. FILIPCZYŃSKI, J. ETIENNE, A. GRABOWSKA, T. WASZCZUK, H. KOWALSKI, M. GRYZIŃSKI, J. STANISŁAWSKI, *An experimental lithotripsy system for the study of shock wave effects*, Archives of Acoustics, **14**, 11–27 (1989).

[6] L. FILIPCZYŃSKI, A. GRABOWSKA, *Deviation of the acoustic pressure to particle velocity ratio from the ϱc value in liquids and in solids at high pressures*, Archives of Acoustics, **14**, 173–179 (1989).

[7] L. FILIPCZYŃSKI, J. ETIENNE, *Capacitance hydrophones for pressure determination in lithotripsy*, Ultrasound in Med. and Biol., **16**, 157–165 (1990).

[8] L. FILIPCZYŃSKI, J. ETIENNE, M. PIECHOCKI, *An attempt to reconstruct the lithotriptor shock wave pulse in kidney. Possible temperature effects*, Ultrasound in Med. and Biol., **18**, 569–577 (1992).

[9] L. FILIPCZYŃSKI, J. ETIENNE, T. KUJAWSKA, *Shock wave pulse pressure after penetration of kidney tissue*, IEEE Transactions on Ultrasonics, Ferroelectrics and Frequency Control, **41**, 130–133 (1994).

[10] L. FILIPCZYŃSKI, J. ETIENNE, G. ŁYPACEWICZ, T. WASZCZUK, *Measurements technique of shock wave pulses at extremely high pressures*, Archives of Acoustics, **21**, 37–51 (1996).

[11] J. FREDERICK, *Ultrasonic Engineering*, J. Willey, New York 1954.

[12] L. KINSLER, A. FREY, *Fundamentals of Acoustics*, p. 166, J. Willey, New York 1962.

[13] P. LEWIN, *Practical implementations and technology of measurement devices*, [in:] Ultrasonic exposimetry, M. ZISKIN, P. LEWIN [Eds.], Boca Raton. CRC Press, London, 1993, pp. 185–215.

[14] I. MALECKI, *Theory of Acoustic Systems* [in Polish], p. 181, PWN, Warszawa 1964.

[15] W.P. MASON, R.N. THOMSON [Eds.], *Physical Acoustics*, p. 382, vol. XIV, Academic Press, New York 1979.

[16] G. MILLER, H. PURSEY, *The field and radiation impedance of mechanical radiators of free source of a semi-infinite isotropic solid*, Proc. R. Soc., London, Ser. A, **223**, 521–541 (1954).